Why Does D_2 Bind Better Than H_2? A Theoretical and Experimental Study of the Equilibrium Isotope Effect on H_2 Binding in a M(η^2-H_2) Complex. Normal Coordinate Analysis of $W(CO)_3(PCy_3)_2(\eta^2\text{-}H_2)$

Bruce R. Bender,*,† Gregory J. Kubas,*,‡ Llewellyn H. Jones,‡ Basil I. Swanson,‡ Juergen Eckert,‡ Kenneth B. Capps,§ and Carl D. Hoff*,§

Contribution from Catalytica Inc., 430 Ferguson Drive, Mountain View, California 94043, Los Alamos National Laboratory, MS-J514, Los Alamos, New Mexico 87545, and the Department of Chemistry, University of Miami, Coral Gables, Florida 33124

Received March 31, 1997[⊗]

Abstract: Vibrational data (IR, Raman and inelastic neutron scattering) and a supporting normal coordinate analysis for the complex *trans*-$W(CO)_3(PCy_3)_2(\eta^2\text{-}H_2)$ (**1**) and its HD and D_2 isotopomers are reported. The vibrational data and force constants support the well-established η^2-bonding mode for the H_2 ligand and provide unambiguous assignments for all metal−hydrogen stretching and bending frequencies. The force constant for the HH stretch, 1.3 mdyn/Å, is less than one-fourth the value in free H_2 and is similar to that for the WH stretch, indicating that weakening of the H−H bond and formation of W−H bonds are well along the reaction coordinate to oxidative addition. The equilibrium isotope effect (EIE) for the reversible binding of dihydrogen (H_2) and dideuterium (D_2) to **1** and **1**-d_2 has been calculated from measured vibrational frequencies for **1** and **1**-d_2. The calculated EIE is "inverse" (**1**-d_2 binds D_2 better than **1** binds H_2), with $K_H/K_D = 0.78$ at 300 K. The EIE calculated from vibrational frequencies may be resolved into a large normal mass and moment of inertia factor (MMI = 5.77), an inverse vibrational excitation factor (EXC= 0.67), and an inverse zero-point energy factor (ZPE = 0.20), where EIE = MMI × EXC × ZPE. An analysis of the zero-point energy components of the EIE shows that the large decrease in the HH stretching frequency (force constant) predicts a large normal EIE but that zero-point energies from five new vibrational modes (which originate from translational and rotational degrees of freedom from hydrogen) offset the change in zero-point energy from the $H_2(D_2)$ stretch. The calculated EIE is compared to experimental data obtained for the binding of H_2 or D_2 to $Cr(CO)_3(PCy_3)_2$ over the temperature range 12−36 °C in THF solution. For the binding of H_2 $\Delta H = -6.8 \pm 0.5$ kcal mol^{-1} and $\Delta S = -24.7 \pm 2.0$ cal mol^{-1} deg^{-1}; for D_2 $\Delta H = -8.6 \pm 0.5$ kcal/mol and $\Delta S = -30.0 \pm 2.0$ cal/(mol deg). The EIE at 22 °C has a value of $K_H/K_D = 0.65 \pm 0.15$. Comparison of the equilibrium constants for displacement of N_2 by H_2 or D_2 in the complex $W(CO)_3(PCy_3)_2(N_2)$ in THF yielded a value of $K_H/K_D = 0.70 \pm 0.15$ at 22 °C.

Introduction

Isotope effects can be extremely informative in mechanistic studies in organometallic chemistry, especially for M−H systems.[1] Yet they often are poorly understood or even perplexing. Unlike the situation in organic chemistry, the ability of metal centers (enzymes included) to reversibly coordinate substrates prior to rate determining steps complicates isotope effect "rules" that were formulated (correctly) by organic chemists. Several reports[2] have appeared concerning deuterium equilibrium isotope effects (EIE's) for the reversible addition of H_2 and D_2 to transition metal centers to form interstitial hydrides/deuterides[2g,h] and, more recently, to various transition-metal complexes in solution to form either metal dihydride/dideuteride complexes[2a−c] (eqs 1 and 2) or dihydrogen/dideuterium complexes (eq 3, left half).[2d−f] Observed EIE's for H_2 versus D_2 addition are usually "inverse" ($K_H < K_D$), showing that metal complexes counterintuitively bind D_2 better than they do H_2.

$$H_2 + \text{"}ML_n\text{"} \underset{}{\overset{K_H}{\rightleftharpoons}} \begin{matrix} H \\ \diagdown \\ ML_n \\ \diagup \\ H \end{matrix} \qquad (1)$$

$$D_2 + \text{"}ML_n\text{"} \underset{}{\overset{K_D}{\rightleftharpoons}} \begin{matrix} D \\ \diagdown \\ ML_n \\ \diagup \\ D \end{matrix} \qquad (2)$$

The discovery[3] of molecular hydrogen complexes[4] altered our understanding of H_2 oxidative addition to transition-metal complexes by showing that H_2 may act as a two-electron ligand without undergoing complete oxidative addition and that such dihydrogen σ complexes are *intermediates* along the pathway of H_2 oxidative addition (eq 3).

$$H_2 + \text{"}ML_n\text{"} \rightleftharpoons \begin{matrix} H \\ | \\ ML_n \\ | \\ H \end{matrix} \rightleftharpoons \begin{matrix} H \\ \diagdown \\ ML_n \\ \diagup \\ H \end{matrix} \qquad (3)$$

Depending on M and L, the H−H separation has been found to vary in a near continuum from 0.82 to 1.6 Å, the point at

* Authors to whom correspondence should be addressed.
† Catalytica Inc.
‡ Los Alamos National Laboratory.
§ University of Miami.
⊗ Abstract published in *Advance ACS Abstracts,* September 1, 1997.

(1) Bullock, R. M. In Transition Metal Hydrides; Dedieu, A., Ed.; VCH Publishers, Inc.: New York, 1992; p 263.
(2) (a) Hostetler, M. J.; Bergman, R. G. *J. Am. Chem. Soc.* **1992**, *114*, 7629. (b) Rabinovich, D.; Parkin, G. *J. Am. Chem. Soc.* **1993**, *115*, 353. (c) Abu-Hasanayn, F.; Krogh-Jespersen, K.; Goldman, A. S. *J. Am. Chem. Soc.* **1993**, *115*, 8019. (d) Gusev, D. G.; Bakhmutov, V. I.; Grushin, V. V.; Vol'pin, M. E. *Inorg. Chim. Acta* **1990**, *177*, 115. (e) Hauger, B. E.; Gusev, D. G.; Caulton, K. G. *J. Am. Chem. Soc.* **1994**, *116*, 208. (f) Bakhmutov, V. I.; Bertran, J.; Esteruelas, M. A.; Lledos, A.; Maseras, F.; Modrego, J.; Oro, L. A.; Sola, E. *Chem. Eur. J.* **1996**, *2*, 815. (g) Wiswall, R. H., Jr.; Reilly, J. J. *Inorg. Chem.* **1972**, *11*, 1691. (h) Luo, W.; Clewley, J. D.; Flanagan, T. B. *J. Phys. Chem.* **1990**, *93*, 6710.

S0002-7863(97)01009-3 CCC: $14.00

which the bond generally is considered to be broken to give a classical dihydride (right side of eq 3).[4,5] This indicates that oxidative addition can be arrested anywhere along the reaction coordinate. A tautomeric equilibrium can even exist in solution between the dihydrogen and dihydride forms in eq 3 in certain cases, including $W(CO)_3(PCy_3)_2(\eta^2\text{-}H_2)$, **1**,[3b] the complex that is the subject of this paper.

We wondered what the deuterium EIE would be for the formation of a dihydrogen complex from H_2 and a metal complex like **1** (left side of eq 3 and eqs 4 and 5 below). This could lead to increased understanding of σ-bond coordination and improved methods for hydrogen isotope separations wherein *molecular* binding is necessary (metal−hydride formation would give isotopic exchange). EIE's have been reported[2d−f] for the binding of H_2 versus D_2 in complexes of the type $MH_x(H_2)L_n$, although these also contained hydride/deuteride ligands, introducing a secondary isotope effect. The data showed that such EIE's were inverse, with typical values of $K_H/K_D = 0.36-0.50$ over a large temperature range. These values are somewhat more "inverse" than those (ca. 0.5) measured and calculated for the binding of H_2/D_2 in dihydride complexes.[2a−c]

The prototype dihydrogen complexes, $W(CO)_3(PR_3)_2(\eta^2\text{-}H_2)$, including **1** (R = Cy), have been extensively characterized by diffraction (X-ray and neutron) and vibrational spectroscopic methods (IR, Raman, and inelastic neutron scattering, INS), as well as by NMR (^1J(HD) NMR coupling constant and T_1 relaxation times). All data concur that ν(HH) and ν(DD) frequencies (hence bond order) are lowered when H_2/D_2 binds to a metal center; this should result in a "normal" equilibrium isotope effect *if changes in the HH(DD) force constant were the major contributor to the EIE*. However, we also anticipated (as elucidated by Krogh-Jespersen and Goldman[2c]) the importance of zero-point energies from new vibrational modes and rotational energy contributions to EIE's when H_2 coordinates.

$$H_2 + \text{"}ML_n\text{"} \underset{}{\overset{K_H}{\rightleftharpoons}} \begin{matrix} H \\ | \\ ML_n \\ | \\ H \end{matrix} \qquad (4)$$

$$D_2 + \text{"}ML_n\text{"} \underset{}{\overset{K_D}{\rightleftharpoons}} \begin{matrix} D \\ | \\ ML_n \\ | \\ D \end{matrix} \qquad (5)$$

Here we have used vibrational modes measured and assigned for **1** and its D_2 analogue, $W(CO)_3(PCy_3)_2(\eta^2\text{-}D_2)$, **1**-$d_2$, to calculate the EIE ($K_H/K_D$) for eq 4 and eq 5 using the formalism of Bigeleisen and Goeppert-Mayer.[6] We have experimentally verified the same EIE for the binding of H_2/D_2 to **1** and **1**-d_2 in THF solution. In addition, we have determined the EIE for the binding of H_2 and D_2 to $Cr(CO)_3(PCy_3)_2$ in THF solution and have determined the temperature dependence of that equilibrium. We also include here the details of a normal coordinate vibrational analysis of **1** and **1**-d_2 plus the related HD complex (**1**-d_1), which we carried out to support vibrational mode assignments and determine force constants and interaction constants for metal−dihydrogen coordination. These data give valuable information relating to the degree of activation of the H−H bond and help explain inconsistencies in the correlation of ν(HH) with electronics at the metal and other properties of H_2 complexes.

Experimental Section

The complexes **1**, **1**-d_1, and **1**-d_2 were prepared as previously described.[3b,c] Infrared spectra were measured for Nujol mulls between CsBr windows and recorded on a Perkin-Elmer 521.[3b] Raman spectra were taken on samples sealed inside glass capillary (melting point) tubes, using the 6471 Å line of a Spectra Physics krypton laser and a SPEX double monochromator. Despite the use of low power (ca. 1 mW) and cooling of the sample to 77 K, partial decomposition slowly took place when the sample was illuminated by the laser beam during the course of the experiments. Surprisingly, the rate of decomposition was higher at 77 K than at 298 K (possibly due to a sample phase change), so spectra were recorded at room temperature.

Inelastic neutron scattering (INS) vibrational data for $W(CO)_3(PCy_3)_2(\eta^2\text{-}H_2)$ were obtained on the Filter Difference Spectrometer at the Manuel Lujan Jr. Neutron Scattering Center of Los Alamos National Laboratory by procedures similar to those published for the P-*i*-Pr_3 analogue.[4e]

Infrared measurements for the experimental determination of equilibria were made on a Perkin Elmer 2000 FTIR spectrometer in a special cell obtained from Harrick Scientific. The stainless steel cell is fitted with germanium windows and attached to a thermostated high-pressure Hoke bomb of 40-mL capacity. Temperature and pressure measurements were made by calibrated thermistor and quartz pressure transducer elements obtained from Omega Scientific and in direct contact with the cell contents. The complexes $W(CO)_3(PCy_3)_2(N_2)$[7] and $Cr(CO)_3(PCy_3)_2$[8] were prepared as previously described. Deuterium, hydrogen, and nitrogen were obtained from Matheson Gas or Liquid Carbonic and were of 99.9995% purity. THF solvent was freshly distilled from Na/benzophenone.

Equilibrium Measurements for the Binding of H_2 and D_2 to $Cr(CO)_3(PCy_3)_2$. A 40-mL Schlenk tube was loaded in a glovebox with 0.2 g of $Cr(CO)_3(PCy_3)_2$ and 30 mL of THF. The solution (25 mL) was loaded under a slight argon pressure into a high-pressure FTIR cell/reaction vessel. After allowing 10−15 min for pressure and temperature equilibration and running of an initial IR spectrum, the cell was filled with D_2 to a total pressure of 6.1 atm. The pressure of D_2 at each temperature was calculated by subtracting out the vapor

(3) (a) Kubas, G. J.; Ryan, R. R.; Swanson, B. I.; Vergamini, P. J.; Wasserman, H. J. *J. Am. Chem. Soc.* **1984**, *106*, 451. (b) Kubas, G. J.; Unkefer, C. J.; Swanson, B. I.; Fukushima, E. *J. Am. Chem. Soc.* **1986**, *108*, 7000. (c) Kubas, G. J. *Inorg. Synth.* **1990**, *27*, 1.

(4) Reviews: (a) Heinekey, D. M.; Oldham, W. J., Jr. *Chem. Rev.* **1993**, *93*, 913. (b) Jessop, P. G.; Morris, R. H. *Coord. Chem. Rev.* **1992**, *121*, 155. (c) Crabtree, R. H. *Acc. Chem. Res.* **1990**, *23*, 95. (d) Kubas, G. J. *Acc. Chem. Res.* **1988**, *21*, 129. (e) Eckert, J. *Spectrochim. Acta A* **1992**, *48A*, 363. Other relevant work: (f) Kubas, G. J.; Nelson, J. E.; Bryan, J. C.; Eckert, J.; Wisniewski, L.; Zilm, K. *Inorg. Chem.* **1994**, *33*, 2954. (g) Andrea, R. R.; Vuurman, M. A.; Stufkens, D. J.; Oskam, A. *Recl. Trav. Chim. Pays-Bas* **1986**, *105*, 372. (h) Upmacis, R. K.; Poliakoff, M.; Turner, J. J. *J. Am. Chem. Soc.* **1986**, *108*, 3645. (i) Zilm, K. W.; Millar, J. M. *Adv. Magn. Opt. Reson.* **1990**, *15*, 163. (j) Kubas, G. J.; Burns, C. J.; Eckert, J.; Johnson, S.; Larson, A. C.; Vergamini, P. J.; Unkefer, C. J.; Khalsa, G. R. K.; Jackson, S. A.; Eisenstein, O. *J. Am. Chem. Soc.* **1993**, *115*, 569. (k) Khalsa, G. R. K.; Kubas, G. J.; Unkefer, C. J.; Van Der Sluys, L. S.; Kubat-Martin, K. A. *J. Am. Chem. Soc.* **1990**, *112*, 3855. (l) Gadd, G. E.; Upmacis, R. K.; Poliakoff, M.; Turner, J. J. *J. Am. Chem. Soc.* **1986**, *108*, 2547. (m) Van Der Sluys, L. S.; Eckert, J.; Eisenstein, O.; Hall, J. H.; Huffman, J. C.; Jackson, S. A.; Koetzle, T. F.; Kubas, G. J.; Vergamini, P. J.; Caulton K. G. *J. Am. Chem. Soc.* **1990**, *112*, 4831. (n) Harman, W. D.; Taube, H. *J. Am. Chem. Soc.* **1990**, *112*, 2261. (o) Kohlmann, W.; Werner, H. *Z. Naturforsch. B* **1993**, *48b*, 1499. (p) Eckert, J.; Albinati, A.; Bucher, U. E.; Venanzi, L. M. *Inorg. Chem.* **1996**, *35*, 1292. (q) Martensson, A.-S.; Nyberg, C.; Andersson, S. *Phys. Rev. Lett.* **1986**, *57*, 2045. (r) Ozin, G. A.; Garcia-Prieto, J. *J. Am. Chem. Soc.* **1986**, *108*, 3099. (s) George, M. W.; Haward, M. T.; Hamley, P. A.; Hughes, C.; Johnson, F. P. A.; Popov, V. K.; Poliakoff, M. *J. Am. Chem. Soc.* **1993**, *115*, 2286. (t) Hodges, P. M.; Jackson, S. A.; Jacke, J.; Poliakoff, M.; Turner, J. J.; Grevels, F.-W. *J. Am. Chem. Soc.* **1990**, *112*, 1234. (u) Klooster, W. T.; Koetzle, T. F.; Jia, G.; Fong, T. P.; Morris, R. H.; Albinati, A. *J. Am. Chem. Soc.* **1994**, *116*, 7677. (v) Hasegawa, T.; Li, Z.; Parkin, S.; Hope, H.; McMullan, R. K.; Koetzle, T. F.; Taube, H. *J. Am. Chem. Soc.* **1994**, *116*, 4352. (w) King, W. A.; Luo, X-L.; Scott, B. L.; Kubas, G. J.; Zilm, K. W. *J. Am. Chem. Soc.* **1996**, *118*, 6782. (x) Moreno, B.; Sabo-Etienne, S.; Chaudret, B.; Rodriguez, A.; Jalon, F.; Trofimenko, S. *J. Am. Chem. Soc.* **1995**, *117*, 7441. (y) Sweany, R. L.; Moroz, A. *J. Am. Chem. Soc.* **1989**, *111*, 3577. (z) Sweany, R. L.; Watzke, D. *Organometallics* **1997**, *16*, 1037.

(5) H−H distances less than 1.6 Å have been measured in over forty complexes by X-ray and neutron diffraction and/or by solution and solid state NMR methods (longer distances exist in classical hydrides).

(6) Bigeleisen, J.; Goeppert-Mayer, M. *J. Chem. Phys.* **1947**, *15*, 261.

(7) Wasserman, H. J.; Kubas, G. J.; Ryan, R. R. *J. Am. Chem. Soc.* **1986**, *108*, 2294.

(8) Gonzalez, A. A.; Mukerjee, S. L.; Chou, S.-J.; Zhang, K.; Hoff, C. D. *J. Am. Chem. Soc*. **1988**, *110*, 4419.

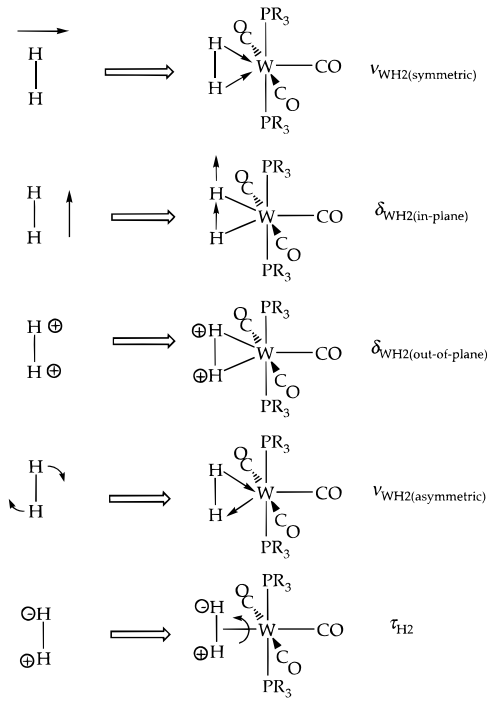

Figure 1. Vibrational modes for the dihydrogen ligand in addition to ν(HH).

pressure of THF and that of argon from the measured pressure. The equilibrium constant was measured at various temperatures in the range 13−36 °C by analysis of the peaks at 1838 cm^{-1} due to Cr(CO)$_3$(PCy$_3$)$_2$(D$_2$) and at 1822 cm^{-1} due to Cr(CO)$_3$(PCy$_3$)$_2$.

Equilibrium Measurements for the Displacement of N$_2$ from W(CO)$_3$(PCy$_3$)$_2$(N$_2$) by H$_2$ and D$_2$. A 6 mM solution of W(CO)$_3$(PCy$_3$)$_2$(N$_2$) in dry O$_2$-free THF was prepared under an atmosphere of N$_2$. This solution was transferred to the high-pressure cell/reactor and allowed to equilibrate at room temperature at a total pressure of 2.25 atm. Following equilibration, saturation of solvent with gas, and running of an initial FTIR spectrum, an additional 2.25 atm of H$_2$ or D$_2$ was added. The ratio of binding was determined from the decrease in the peak at 2117 cm^{-1} attributed to coordinated N$_2$ in W(CO)$_3$(PCy$_3$)$_2$(N$_2$) when exposed to either H$_2$ or D$_2$. At 22 °C a clear preference for binding of D$_2$ versus H$_2$ was seen in all experiments, and a value of $K_H/K_D = 0.70 \pm 0.15$ was measured for the net binding of H$_2$ or D$_2$ to W(CO)$_3$(PCy$_3$)$_2$ relative to N$_2$ at 22 °C.

Results

Vibrational Frequency Assignments and Force Field for W(CO)$_3$(PCy$_3$)$_2$(H$_2$) (1). When diatomic H$_2$ combines with a metal−ligand fragment to form a molecular hydrogen complex like **1** (eq 4), five "new" vibrational modes are created (in addition to ν(HH)) which are related to the "lost" translational and rotational degrees of freedom for H$_2$ (Figure 1). Six fundamental vibrational modes for **1** are expected to be formally isotope sensitive, as observed. As described earlier,[3b] the infrared spectra of solid W(CO)$_3$(PCy$_3$)$_2$(η^2-H$_2$) (**1**), W(CO)$_3$(PCy$_3$)$_2$(η^2-HD) (**1**-d_1), and W(CO)$_3$(PCy$_3$)$_2$(η^2-D$_2$) (**1**-d_2) display many overlapping vibrational frequencies, but a substantial number of them show isotopic shifts (Figures 2 and 3). On the basis of isotope shifts and force field calculations, the observed frequencies have been assigned to vibrational modes as shown in Table 1. These do not include frequencies that are associated with the phosphine ligands nor W−P modes which would be expected to occur at low frequencies (<300 cm^{-1}) and could not be located with any certainty.

There is significant mixing between the modes associated with the H$_2$ and CO ligands, and there is less available frequency data than that needed for a fully determined normal coordinate

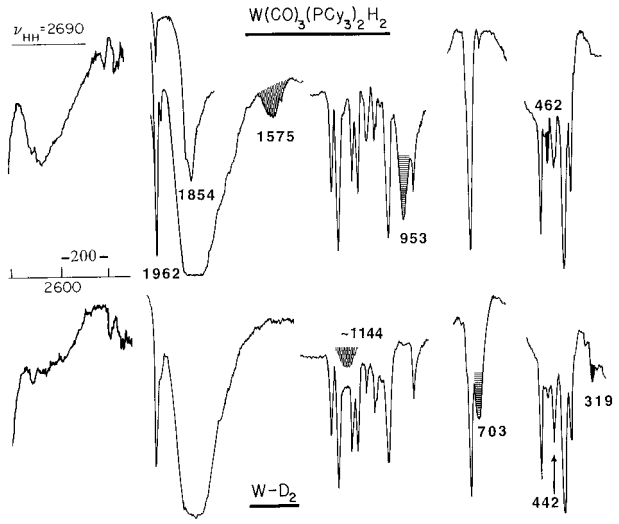

Figure 2. Infrared spectra of Nujol mulls of **1** (upper) and **1**-d_2 (lower). The ν(HH) region was recorded for the perdeuteriophosphine species.

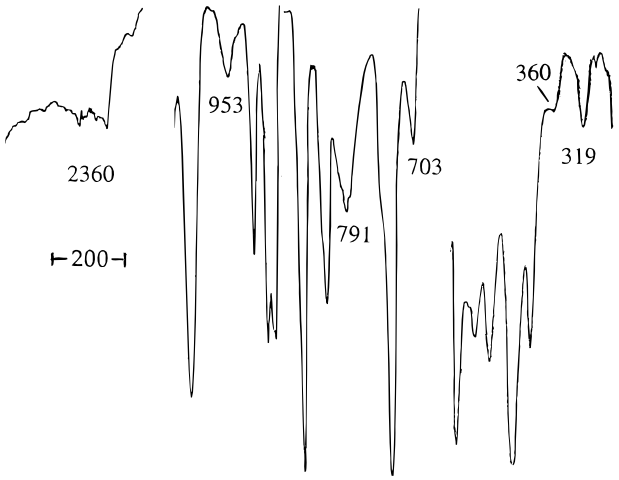

Figure 3. Infrared spectrum of Nujol mull of **1**-d_1. The broad ν(HH) signal at 2360 cm^{-1} is superimposed over sharper atmospheric CO$_2$ bands. The shoulder at 360 cm^{-1} is ascribed to δ(WHD) in-plane.

analysis (a not uncommon situation). However, because of the large isotopic shifts resulting upon deuteration of the H$_2$ ligand, we are confident of the assignment of the modes associated with the η^2-H$_2$. Importantly in this regard, the HD complex shows W−η^2-HD bands *intermediate* in frequency to those of the HH and DD complexes rather than as superimpositions of M(H)$_2$ and M(D)$_2$ bands as found for classical hydride−deuteride complexes M(H)(D).

The single vibrational mode for H$_2$, ν(HH), remains intact, but is shifted to much lower frequency, 2690 cm^{-1}, compared to free H$_2$.[3] It is not formally forbidden in the IR of H$_2$ complexes, but is polarized along the direction of the M−H$_2$ bond in highly symmetric complexes. Therefore, intensity arises only from coupling of ν(HH) with other modes of the same symmetry such as ν_s(MH$_2$) or ν(CO) if CO is present. Thus ν(HH) is almost always very weak, and in **1** could only be clearly observed in the IR by using thick Nujol mulls of the complex containing perdeuteriophosphine ligands to remove interference from the CH bands of the cyclohexyl groups (Figure 2). The large breadth of the absorption is ascribed to rapid hindered rotation of the H$_2$ ligand about the W−H$_2$ axis[4e] or some other motion/behavior that dephases ν(HH), "hot" band contributions, and a flat rotational potential.[9]

Table 1. Observed[a] and Calculated Vibrational Frequencies (cm^{-1}) and Mode Assignments for **1**, **1**-d_2, and **1**-d_1

method/ intensity	**1** obsd	**1** calcd	**1**-d_2 obsd	**1**-d_2 calcd	**1**-d_1 obsd	**1**-d_1 calcd	symmetry C_{2v}/C_s	assignment
IR, w	2690	2692.1	~1900[b]	1909.9	2360	2357.8	A_1/A'	ν(HH)
IR, R, s	1962	1965.3	1962	1965.4	1962	1965.3	A_1/A'	$\nu(CO)_{eq}$
IR, R, vs	1857[c]	1854.3	1847[c]	1849.4	1853[c]	1853.6	A_1/A'	$\nu(CO)_{ax}$
IR, R, m	953	949.0	703	703.1	791	799.8	A_1/A'	$\nu_s(WH_2)$
IR, R, w	558	546.7	551	544.5	553	545.8	A_1/A'	$\delta(WCO)_{eq}$
R, s	465	464.1	450	443.4		459.9	A_1/A'	$\nu(WC)_{ax} + \nu_s(WH_2) + \nu$(HH)
R, s	452	452.2	456	455.6		451.0	A_1/A'	$\nu(WC)_{eq}$
IR, w	1575	1574.7	~1144	1136.1	~1360	1357.9	B_1/A'	$\nu_{as}(WH_2)$
IR, s	623	626.8	612	612.2	614	617.1	B_1/A'	$\delta(WCO)_{ax}$
R, w	527	523.4	522	523.0	–	523.2	B_1/A'	$\delta(WCO)_{eq}$
IR, w	462[d]	456.2	319	326.0	360	368.7	B_1/A'	$\delta(WH_2)_{in-plane}$[e]
R, w	400	400.0	413	413.0			B_2/A''	$\nu_{as}(WC) + \delta(WH_2)_{out-of-plane} + \delta(WCO)$
INS,[f] IR, w	640[g]	640.0	442[h]	442.0			B_2/A''	$\delta(WH_2)_{out-of-plane}$
INS, m	385 (325)[i]						A_2/A''	$\tau(WH_2)$

[a] Resolution: 2 cm^{-1}. [b] Raman; very weak and broad. [c] Raman frequencies. [d] Also observed in INS. [e] This mode shows a greater observed isotope shift than calculated. We believe it arises from the δ (WH_2) in-plane rocking coordinate coupled strongly with other coordinates. [f] INS = Inelastic neutron scattering. [g] Observed in INS only. [h] Observed in IR only. [i] Split mode (see ref 4e).

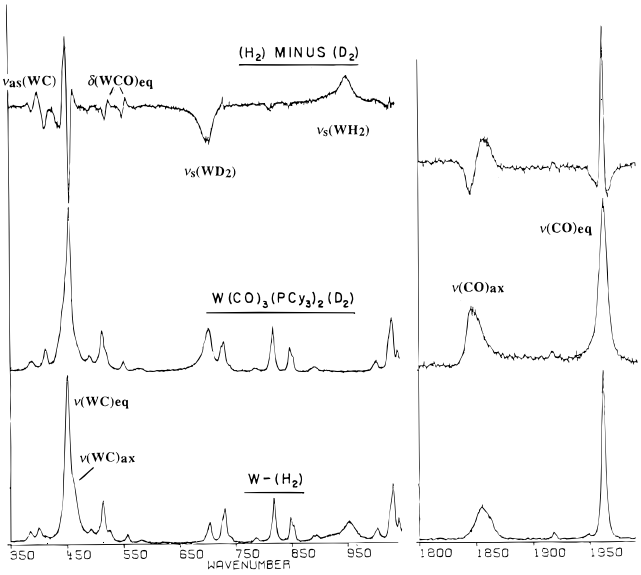

Figure 4. Raman spectra of **1** and **1**-d_2 and difference spectrum.

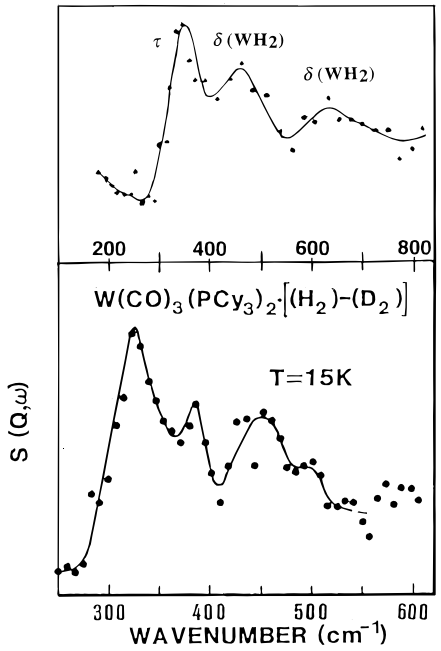

Figure 5. Inelastic neutron scattering (INS) spectra of **1** at 15 K obtained as difference spectra by subtracting the spectrum of **1**-d_2 from **1** (scattering from deuterium is negligible; only bands due to the H_2 ligand appear). The lower spectrum with higher resolution shows splitting in the torsional mode (385/325 cm^{-1}).

ν(HD) was observed in the IR as a weak broad band at ca. 2360 cm^{-1} (Figure 3) in **1**-d_1, but ν(DD) was obscured by ν(CO) in **1**-d_2. However, Raman spectra of **1**-d_2 showed a very broad, barely visible feature centered near 1900 cm^{-1} that apparently mixes with $\nu(CO)_{ax}$. This results in a shift of 10 cm^{-1} to lower energy for the latter on going from the H_2 complex to the D_2 complex (Figure 4). The asymmetry in the $\nu(CO)_{ax}$ peak for **1**-d_2 also suggests the presence of ν(DD) as an underlying feature, the intensity of which is enhanced by the mixing (ν(HH) was not observed in Raman spectra, apparently because it is not so enhanced and is thus too weak to be seen in these experiments). The W−H_2 stretches were observed clearly in the IR at 1575 ($\nu_{as}(WH_2)$) and 953 cm^{-1} ($\nu_s(WH_2)$), but in the Raman only $\nu_s(WH_2)$ was seen. $\nu_{as}(WD_2)$ and ν_{as}(WHD) were partially obscured, and their frequencies could only be estimated. **1**-d_1 contained some **1** and **1**-d_2 because slow isotopic scrambling occurs, even in the solid state. This is obvious in Figure 3 in the $\nu_s(WH_2)$ and δ (WH_2) in-plane regions which show peaks due to all three isotopomers.

The torsional mode, $\tau(WH_2)$, was located in the inelastic neutron scattering (INS) difference spectrum (Figure 5) as a split mode at 385 and 325 cm^{-1} due to transitions to two split excited librational states ($J = 1, 2$).[4e] The two WH_2 deformational modes at 640 and 462 cm^{-1} were also seen in the INS, as broad features. The deformation around 640 cm^{-1} was obscured in the IR but was seen to be shifted to 442 cm^{-1} in the IR for the D_2 isotopomer. Several other metal−ligand modes also show small shifts to higher or lower wavenumber upon deuterium substitution due to vibrational coupling between modes which belong to the same symmetry block and which are close in energy. This is especially obvious in the IR spectra[3b] of **1** and **1**-d_2 near 625 cm^{-1} and Raman spectra in the region below 650 cm^{-1} (Figure 4). For example, a band at 400 cm^{-1} due mainly to ν_{as}(WC) shifts 13 cm^{-1} to *higher* frequency for the D_2 complex, presumably because of mixing with $\delta(WD_2)_{out-of-plane}$. Such shifts have also been observed in other complexes containing both H_2 and CO ligands.[4h,z]

Normal Coordinate Analysis of 1, 1-d_2, 1-d_1, and Simplified Model Complexes. It is clear that the Cy (cyclohexyl)

(9) Turner, J. J.; Poliakoff, M.; Howdle, S. M.; Jackson, S. A.; McLaughlin, J. G. *Faraday Discuss.* **1988**, *86*, 271.

Scheme 1

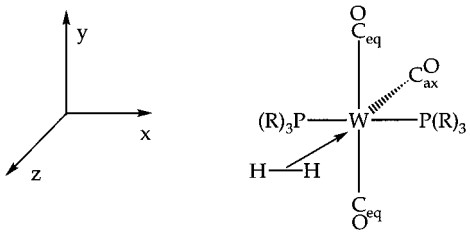

1

Table 2. Force Constants (mdyn/Å) for Hydrogen-Related Modes in W(CO)$_3$P$_2$(H$_2$) and Triatomic Model Complex

	W(CO)$_3$P$_2$(H$_2$)	W(H$_2$)
F_{HH}	1.32	1.46
$F_{WH(s)}$	1.46	
$F_{WH(as)}$	1.42	
F_{WH}	1.44	1.43
$F_{WH,WH'}$	0.02	−0.05
$F_{HH,WH}$	0.67	0.62

groups should not show formal HH, HD, DD isotope shifts, nor should they be significantly coupled to vibrations other than Cy and P−Cy modes; therefore for force field calculations we treated only the "W(H$_2$)(CO)$_3$P$_2$" fragment. The symmetry of that fragment is C_{2v}, with two H atoms, two P atoms, the axial CO group, and W defining one (*xz*) plane; the three CO groups and W define the other (*yz*) plane as in Scheme 1. However, to include the HD species, the symmetry is reduced to C_s.

We have assigned the observed IR and Raman frequencies to the A′ block of C_s; 11 modes of this symmetry were observed (WP modes were not located). This includes 7 modes of A_1 symmetry and 4 B_1 modes of C_{2v} symmetry for the HH and DD species. To carry out the force constant calculations it was necessary to include input force constants for all modes, including those unobserved such as those for W−P (a force constant of 2−3 was assumed and all interaction coordinates, *F*(WP,*x*) were set to zero). There are 10 A_1 modes, 7 B_1 modes, 3 A_2 modes, and 7 B_2 modes; the number of force constants required for each symmetry block is $n(n+1)/2$, where n is the number of frequencies in that block. This means there are 55 general quadratic force constants to fit 7 observed A_1 modes, 28 to fit 4 B_1 modes, etc. Obviously a large number of force constants had to be fixed for the calculations. For these constants we assumed values that seemed reasonable based on experience with other systems such as W(CO)$_6$.[10] Several calculations were performed, and the values of some of the "fixed" constants were varied to improve the fit. The solution arrived at is given in Table 1. The agreement of observed and calculated frequencies is off by several wavenumbers in some cases, which is not surprising considering the necessary approximations. Overall, the analysis suffices to assign the observed vibrational modes for **1** and its isotopomers as well as provide meaningful force constants for the dihydrogen-related modes.

The force constants given in Table 2 that pertain to the H$_2$ ligand are extremely valuable in gaining understanding of the W−H$_2$ bonding interactions. The first and most important mode to consider is the HH stretch. The value of 1.3 mdyn/Å is much smaller than the value for free H$_2$ (5.7 mdyn/Å).[11] The ratio of the square of frequencies for bound and free H$_2$, $(2690/4395)^2 = 0.37$, would lower 5.7 to 2.1 mdyn/Å. However, we see that the HH stretch has considerable WH stretch character so it cannot be treated as an isolated HH mode. The low value of F_{HH} would suggest a longer HH distance, *ca.* 0.94 Å,[12] than either the value of 0.82 Å observed by neutron diffraction[3b] in W(CO)$_3$(P-*i*-Pr$_3$)$_2$(H$_2$) or 0.89 Å determined by solid state NMR[4i] for both the R = *i*-Pr and Cy species. Thus ν(HH) is not a reliable predictor of HH bond length for molecular hydrogen complexes.[13]

Table 3. Force Constants and Interaction Constants for CO-Related Modes (mdy/Å for stretching coordinates; mdyn·Å/rad^2 for bending coordinates)

coordinate		coordinate	
CO$_{eq}$ + CO, CO′	15.07	WH$_2$(s), WC$_{ax}$	0.70
CO$_{ax}$	13.38	WH$_2$(s), WCO (s)	0.1
WC$_{eq}$ + WC, WC′	3.54	CO$_{eq}$, CO$_{ax}$	0.28
WC$_{ax}$	4.00	CO$_{eq}$, WC$_{eq}$	0.6
WCO$_{ax}$	1.18	CO$_{ax}$, WC$_{ax}$	0.75
WCO$_{eq}$(as)	0.7	WC(s), WC$_{ax}$	0.1
WCO$_{eq}$(s)	0.8	WH$_2$(as), WCO$_{eq}$(s)	0.05
torsion (τ)	0.12	WH$_2$(as), WCO$_{ax}$	0.48
WH$_2$(s), CO$_{ax}$	0.25		

The WH stretching constant is surprisingly as large as that for the HH stretch, and the WH, WH′ interaction is negligible. The HH, HW interaction is very large (0.67 mdyn/Å), indicating that stretching the HH bond leads to strengthening of the HW bonds, and vice versa.

The WC stretching force constants (Table 3) are quite large relative to those for W(CO)$_6$. Thus for the equatorial WC bonds, $F_{WC} + F_{WC,WC'} = 3.54$ mdyn/Å compared to 2.92 mdyn/Å for W(CO)$_6$.[10] This is reasonable as the respective distances are 2.01[14] and 2.06 Å.[15] The axial (trans to H$_2$) WC stretching constant is even greater (4.0 mdyn/Å), in accord with its shorter distance (1.99 Å). This stretching mode is noticeably weakened in the D$_2$ isotopomer (465 cm^{-1} for **1** versus 450 cm^{-1} for **1**-d_2). This might reflect a greater trans influence for D$_2$ versus H$_2$ (an "electronic" isotope effect); however, we might then expect a corresponding increase in νCO for **1**-d_2 (a weakening of WC should be accompanied by a decrease in W→CO π-back-bonding). The observed *decrease* in the axial WC stretching frequency for **1**-d_2 no doubt arises because it is coupled with the symmetric W−D stretch and the D−D stretch.

The equatorial C−O stretching constant is about 15 mdyn/Å compared to ca. 16 for W(CO)$_6$. The value for the axial CO stretch is 13.4 mdyn/Å. The increase in MC bond strength and decrease in CO bond strength is consistent with stronger M→CO π-back-bonding when there are fewer π-acceptor groups available, particularly opposite the CO. Also in accord with this notion, the M−C−O bending constants are greater than for W(CO)$_6$. They are 0.8 mdyn·Å/rad^2 for the equatorial and 1.3 for the axial MCO, compared to <0.6 for W(CO)$_6$.

There is a weak Raman band at 400 cm^{-1} which shifts *upward* to 413 cm^{-1} for **1**-d_2 (Table 1). Our calculations

(10) Jones, L. H.; McDowell, R. S.; Goldblatt, M. *Inorg. Chem.* **1969**, *8*, 2349.

(11) Levine, I. N. *Molecular Spectroscopy*; Wiley: New York, 1975; p 160

(12) An empirical correlation between bond length and force constant, known as Badger's rule, $k_e = b/(r_e - a)^3$, would predict an HH bond length of *ca.* 0.94 Å: Badger, R. M. *J. Chem. Phys.* **1934**, *2*, 128.

(13) See ref 4e and the Discussion section. A similar situation arises for metal−*ethylene* complexes: ν(CC) is not a reliable parameter of CC bond length because of normal mode coupling to same-symmetry C$_2$H$_4$ wagging and scissoring modes: Anson, C. E.; Sheppard, N.; Powell, D. B.; Bender, B. R.; Norton, J. R. *J. Chem. Soc., Faraday Trans.* **1994**, *90*, 1449 and references therein.

(14) Kubas, G. J.; Ryan, R. R.; Wasserman, H. J. Unpublished data. The H$_2$ ligand was obscured by a CO ligand, which is disordered across the center of symmetry located at the tungsten center. However, the overall geometry of the complex was similar to that for the *i*-Pr analogue wherein the H$_2$ was located.

(15) Arnesen, S. P.; Seip, H. M. *Acta Chem. Scand.* **1966**, *20*, 2711.

Table 4. Frequency Fit for the Triatomic $W(H_2)$ Model Complex (cm^{-1})

HH		DD		HD	
obsd	calcd	obsd	calcd	obsd	calcd
2690.0	2691.2	~1900	1905.8	2360.0	2358.1
1575.0	1576.9	~1140	1115.7	1350.0	1347.5
953.0	964.6	703.0	685.2	791.0	791.5

indicate that this mode arises from the antisymmetric WC stretch strongly coupled with the WD_2 out-of-plane deformation (wagging) coordinate, which leads to the upward shift for **1**-d_2. Coupling to the two out-of-plane WCO bending coordinates is also present. For the (A_2-symmetry) torsion mode, we calculate a constant of 0.12 mdyn·Å/rad^2 with the torsion described by changes in CWH angles.

We have also calculated stretching force constants for an isolated WH_2 group using the frequencies observed for the HH and WH stretches. The results are shown in Table 2 for comparison with the more complete treatment. Surprisingly the agreement is quite good, suggesting that one can do rather well with the simplified treatment, though it does not tell us about the rest of the molecule. The frequency agreement for the simplified triatomic treatment is shown in Table 4. It is seen to be rather poor by comparison, particularly for the symmetric WH_2 stretch. One can obtain better agreement by including rather large anharmonicity corrections for the WH stretches; however, the more complete treatment without anharmonicity is perhaps more appropriate as the many isotope shifts of a few wavenumbers indicate significant coupling of H coordinates with non-H coordinates.

Calculated Deuterium Equilibrium Isotope Effect (EIE). Division of eq 4 by eq 5 (with $ML_n = W(CO)_3L_2$) leads to eq 6, and K_H/K_D is a direct measure of the deuterium equilibrium isotope effect (EIE).

$$H_2 + \begin{matrix} D \\ | \\ D \end{matrix}\!\!-\!\!W(CO)_3L_2 \quad \underset{}{\overset{K_H/K_D}{\rightleftharpoons}} \quad D_2 + \begin{matrix} H \\ | \\ H \end{matrix}\!\!-\!\!W(CO)_3L_2 \qquad (6)$$

1-d_2 **1**

K_H/K_D in eq 6 may be calculated from vibrational data if all isotopically sensitive frequencies for the four species are known or can be reliably estimated. The electronic potentials on both sides of eq 6 are identical (with the Born−Oppenheimer and harmonic oscillator assumptions), and the only sources of an EIE deviation from unity are mass-related, i.e., translational, rotational, and vibrational. Thus the EIE in eq 6 may be calculated from molecular translational, rotational, and vibrational partition function ratios as described in the general treatment of equilibrium isotope effects by Bigeleisen and Goeppert-Mayer.[6]

$$\mathrm{EIE} = \mathrm{MMI} \times \mathrm{EXC} \times \mathrm{ZPE} \qquad (7)$$

The calculated EIE is the product of three factors[16] (the usual symmetry factor cancels for this case). They are a rotational and translational factor containing the reduced (classical) rotational and translational partition function ratios of isotopic species (abbreviated MMI, eq 8), a factor accounting for contributions from excitations of vibrational energy levels (abbreviated EXC, eq 9), and a factor comprising zero-point energy contributions (abbreviated ZPE, eq 10).

$$\mathrm{MMI} = \left(\frac{Q_{tr}^{A*}Q_{rot}^{A*}}{Q_{tr}^{A}Q_{rot}^{A}}\right)\left(\frac{Q_{tr}^{B}Q_{rot}^{B}}{Q_{tr}^{B*}Q_{rot}^{B*}}\right) \qquad (8)$$

$$\mathrm{EXC} = \frac{\prod_{i}^{3N-6} \frac{1-\exp(-\mu_i)}{1-\exp(-\mu^*_i)}}{\prod_{j}^{3N-6} \frac{1-\exp(-\mu_j)}{1-\exp(-\mu^*_j)}} \qquad (9)$$

$$\mathrm{ZPE} = \frac{\prod_{i}^{3N-6} \frac{\exp(\mu_i/2)}{\exp(\mu^*_i/2)}}{\prod_{j}^{3N-6} \frac{\exp(\mu_j/2)}{\exp(\mu^*_j/2)}} \qquad (10)$$

As a first approximation, we assumed that changes in mass and moments of inertia between **1** and **1**-d_2 are negligible (i.e., that both the translational and rotational partition function ratios for **1** and **1**-d_2 are equal to 1) and calculated the MMI factor from the appropriate mass and moment of inertia ratios of H_2 and D_2 alone.[17] The classical description of the translational, $(2\pi M k_B T)^{3/2}/h^3$, and rotational, $8\pi^2 I k_B T/\sigma h^2$ (linear molecule), energies[18,19] gives ratios of 2.83 and 2.00, respectively, leading to an MMI term of 5.66.[2c]

We may independently calculate the MMI term for the EIE in eq 6 from measured vibrational frequencies for **1**, **1**-d_2, H_2, and D_2, using the Teller-Redlich product rule[20] (shown in its most concise form in eq 11). This important theorem allows the ratios of molecular masses and moments of inertia of isotopically related species to be expressed as a product of atomic masses and vibrational frequencies.

$$\left(\frac{M^*}{M}\right)^{3/2} \times \left(\frac{I_A^* I_B^* I_C^*}{I_A I_B I_C}\right)^{1/2} = \prod_{j}^{N}\left(\frac{m^*_j}{m_j}\right)^{3/2} \times \prod_{i}^{3N-6}\frac{\nu^*_i}{\nu_i} \qquad (11)$$

In eq 11, I_A, I_B, and I_C are the principal molecular moments of inertia, M and M^* are molecular masses, and m_j and m^*_j are atomic masses (asterisks denote the heavier isotope). For the linear molecules H_2 and D_2, the vibrational product contains only one frequency, and the ratio of moments of inertia contains one less moment of inertia.

Division of eq 11 for isotopic dihydrogens by the corresponding eq 12 for **1** and **1**-d_2 yields eq 12 (the products of *atomic* masses on both sides of eq 6 are the same and therefore are eliminated), therefore the MMI factor (eq 8) may be replaced with the vibrational product (VP) factor (eq 12), which accounts for the mass and moment of inertia ratios needed to calculate the EIE.

(16) We have used the equations presented by: McLennan, D. J. *Isotopes in Organic Chemistry*; Buncel, E., Lee, E., Eds.; Elsevier: New York, 1987; Vol. 7, Chapter 6, pp 393-480.

(17) We have assumed that the solution translational and rotational partition function ratios for H_2 and D_2 resemble those in the gas phase; the rotation of H_2 appears to be only slightly hindered in aqueous solution: Taylor, D. G., III; Strauss, H. L. *J. Chem. Phys.* **1989**, *90*, 768. (b) Hunter, J. E., III; Taylor, D. G., III; Strauss, H. L. *J. Chem. Phys.* **1992**, *97*, 50.

(18) In eqs 9 and 10, $\mu_{i,j} = hc\nu_{ij}/kT$, where $\nu_{i,j}$ are vibrational frequencies (in cm^{-1}); c is the speed of light, $c = 2.997924 \times 10^{10}$ cm/s; h is Planck's constant, $h = 6.626176 \times 10^{-34}$ J s; k is Boltzmann's constant, and $k = 1.380662 \times 10^{-23}$ J/K. All values of physical constants were taken from: *Handbook of Chemistry and Physics*, 62nd ed.; Weast., R. C., Ed.; CRC Press: Boca Raton, FL, 1981−82; Table F-203.

(19) Moelwyn-Hughes, E. A. *Physical Chemistry;* Pergamon Press: New York, 1961; pp 427−1007.

(20) Melander, L.; Saunders, W. H. *Reaction Rates of Isotopic Molecules*; Wiley: New York, 1980; p 20.

$$\mathrm{VP} = \frac{\dfrac{\nu_{\mathrm{D}_2}}{\nu_{\mathrm{H}_2}}}{\displaystyle\prod_i^{3N-6} \frac{\nu_i^{\mathbf{1}-d_2}}{\nu_i^{\mathbf{1}}}} = \frac{Q_{\mathrm{tr}}^{\mathrm{D}_2} Q_{\mathrm{rot}}^{\mathrm{D}_2}}{Q_{\mathrm{tr}}^{\mathrm{H}_2} Q_{\mathrm{rot}}^{\mathrm{H}_2}} \times \frac{Q_{\mathrm{tr}}^{\mathbf{1}-\mathrm{H}_2} Q_{\mathrm{rot}}^{\mathbf{1}-\mathrm{H}_2}}{Q_{\mathrm{tr}}^{\mathbf{1}-\mathrm{D}_2} Q_{\mathrm{rot}}^{\mathbf{1}-\mathrm{D}_2}} = \mathrm{MMI} \qquad (12)$$

The vibrational product in the denominator on the left side of eq 12 is a product over all vibrational modes for isotopomers of both molecules; however, several modes common to **1** and **1**-d_2 will exactly cancel in eqs 11 and 12 *if they are not isotopically sensitive* and may thus be omitted from further consideration. We have used this to advantage by omitting the cyclohexyl mode frequencies for **1** and **1**-d_2 that are not isotope sensitive.

For the VP factor in eq 12 we have used 14 normal vibrational modes measured and assigned for **1** and **1**-d_2 (Table 1). We used an average value of 355 cm^{-1} for the split torsion mode and have calculated the torsional mode frequency (251 cm^{-1}) for **1**-d_2 from reduced mass considerations. The calculated VP factor is 5.77 and agrees well with the value (5.66) calculated from the mass and moment of inertia ratios of H_2 and D_2 alone. This agreement is also an *independent* check of the accuracy of the vibrational frequencies (but not assignments) of **1** and **1**-d_2. The calculated VP factor (which represents translational and rotational contributions to eq 6 (MMI) is large and "normal" (5.77); this factor is a direct consequence of the significant mass and moment of inertia ratios of D_2 and H_2 (eq 11).

The calculated EIE value ($K_H/K_D = 0.78$) for eq 6 is modestly inverse at 300 K. The individual EXC and ZPE factors for the single $H_2(D_2)$ mode and six $W(H_2)$ modes were calculated and the results are gathered in Table 5. For convenience of discussion, we have separated the six normal modes of the "W-(H_2)" fragment from the other modes which show slight but significant isotope shifts (Table 6).

It should be pointed out that the overall calculated EIE is independent of individual mode assignments for **1** and **1**-d_2. Because the factors comprising the product terms in eqs 9−12 commute for a given species, the calculated EIE is independent of assignments. Mode assignments, however, are useful for interpreting the "origin" of the EIE in terms of changes in particular vibrational frequencies, thus each assignment is shown with its individual contributions to the EXC and ZPE factors. These results give insight into the origin of the calculated EIE for the complexation of dihydrogen isotopes to W(CO)$_3$L$_2$.

The change in zero-point energy for the HH(DD) stretching mode contributes a large "normal" factor to the total EIE as expected; the calculated ZPE contribution would predict an EIE of *ca.* 3.2 for eq 6 if changes in the HH(DD) stretching force constant were the only contributor to the EIE. The five "new" vibrational normal modes of **1** and **1**-d_2 all contribute modest inverse EXC and ZPE factors to the calculated EIE for eq 6 (last two columns in Table 5). When multiplied together, these modest inverse EXC and ZPE contributions from the five "new" vibrational modes collectively overcome the strong "normal" ZPE component from the νHH stretch (and the "normal" MMI factor), and predict an overall "inverse" EIE of 0.78 at 300 K.

Two modes contribute significant inverse EXC factors to the overall EIE. They are the low-frequency a_2-symmetry torsional and the b_1-symmetry in-plane deformation (wag) modes (illustrated in Scheme 1); these low-frequency modes are significantly more populated at 300 K (Boltzmann excitation) for **1**-d_2 than for **1**.

Experimental Determination of the EIE for M(CO)$_3$(PCy$_3$)$_2$, M = Cr and W. Equilibria for the binding of H_2 and D_2 were determined in a similar fashion to that described in an earlier report.[21] For the chromium complex, Cr(CO)$_3$(PCy$_3$)$_2$, the equilibrium shown in eq 13 is rapidly established under moderate pressures of H_2 (1−10 atm) in THF solution:

$$\mathrm{Cr(CO)_3(PCy_3)_2(soln)} + \mathrm{H_2} \rightleftharpoons \mathrm{Cr(CO)_3(PCy_3)_2(H_2)(soln)} \qquad (13)$$

$$\mathrm{Cr(CO)_3(PCy_3)_2(soln)} + \mathrm{D_2} \rightleftharpoons \mathrm{Cr(CO)_3(PCy_3)_2(D_2)(soln)} \qquad (14)$$

Because oxidative addition does not occur for the chromium complex, equilibrium data for eqs 13 and 14 do not incorporate the dihydrogen/dihydride equilibrium shown in eq 3. Experimental data for the equilibrium constant (in atm^{-1}) are shown in Figure 6. These data also incorporate earlier data for the dihydrogen case. Thermochemical parameters for binding of H_2 (eq 13) are $\Delta H = -6.8 \pm 0.5$ kcal mol^{-1} and $\Delta S = -24.7 \pm 2.0$ cal mol^{-1} deg^{-1}. For the binding of D_2 (eq 14) $\Delta H = -8.6 \pm 0.5$ kcal mol^{-1} and $\Delta S = -30.0 \pm 2.0$ cal mol^{-1} deg^{-1}. The data for the H_2 case differ slightly from those reported earlier:[21] $\Delta H = -7.3$ kcal mol^{-1} and $\Delta S = -25.6$ cal mol^{-1} deg^{-1} for H_2. The principal reason for this is that the earlier data were measured by taking the pressure readings directly from the pressure gauge without correcting for solvent and atmospheric pressure. The current data in Figure 6 incorporate both the new data and earlier data corrected for pressure.

The EIE value for the tungsten complex could not be measured directly because there is near quantitative uptake of H_2 or D_2 gas at pressures near 1 atm, presumably due to stronger $W(H_2)$ bonding. The highly air sensitive nature of the agostic complex W(CO)$_3$(PCy$_3$)$_2$ also limits the accuracy of data at low partial pressures of H_2. The equilibrium shown in eq 15 provides a means of determining accurate EIE values:

$$\mathrm{W(CO)_3(PCy_3)_2(N_2)(soln)} + \mathrm{H_2(gas)} \rightleftharpoons \mathrm{W(CO)_3(PCy_3)_2(H_2)(soln)} + \mathrm{N_2(gas)} \qquad (15)$$

Spectroscopic measurements with calibrated H_2/N_2 and D_2/N_2 gas mixtures allowed determination that $K_H/K_D = 0.70 \pm 0.15$ in THF solvent at 22 °C. This value refers to the "net" binding of H_2 (vs D_2) and does not distinguish between the tautomeric forms (eq 3). Because the equilibrium in eq 3 displays temperature dependence (and this could be different for H_2 and D_2, vide infra), no attempt was made to measure the temperature dependence of the tungsten equilibrium constant.

Discussion

Vibrational Analysis of Dihydrogen Complexes. The complete set of six vibrational modes has been identified only in the first and most intensely-studied H_2 complex, W(CO)$_3$(PR$_3$)$_2$(H_2) (R = Cy, *i*-Pr).[22] The main reason for this is that all but $\nu_s(MH_2)$ are weak in the IR and Raman and most of the bands tend to be obscured by other ligand modes. Also, $\tau(H_2)$, and $\delta(MH_2)_{\mathrm{out-of-plane}}$ have been observed only by inelastic neutron scattering (INS) methods. The frequency of most interest ν(HH) varies tremendously, but is often near the CH stretch region, the worst possible position because most ancillary ligands contain CH bonds. Nevertheless, it has been observed in about 20 complexes in the range 2080−3200 cm^{-1}, which is

(21) Gonzalez, A. A.; Hoff, C. D. *Inorg. Chem.* **1989**, *28*, 4295.

(22) For general discussion of the vibrational spectra of $M(H)_2$ and $M(H_2)$ species see: Sweany, R. L. *Transition Metal Hydrides*; Dedieu, A., Ed.; VCH Publishers: New York, 1991; pp 65−101.

Table 5. Equilibrium Isotope Effect Contributions from Individual Modes for $H_2(D_2)$ Complexation at $T = 300$ K

mode (sym)	$H_2(D_2)$ (cm^{-1})	**1**(**1**-d_2) (cm^{-1})	EXC	ZPE
$\nu(H_2)$ (A_1)	4395 (3118)	2690 (1900)	1.000	3.215
$\nu(WH_2)$ (A_1)		953 (703)	0.976	0.549
$\nu(WH_2)$ (B_1)		1575 (1144)	0.996	0.356
$\delta(WH_2)$ (B_2)		640 (442)	0.923	0.622
$\delta(WH_2)$ (B_1)		462 (319)	0.879	0.710
$\tau(WH_2)$ (A_2)		355 (251)	0.856	0.780
			$\prod$ EXC = 0.675	$\prod$ ZPE = 0.216

Table 6. Equilibrium Isotope Effect Contributions From Additional Modes (300 K)

mode	**1**(**1**-d_2) (cm^{-1})	EXC	ZPE
$\nu(CO_{eq})$	1962 (1963)	1.000	1.000
$\nu(CO_{ax})$	1857 (1847)	1.000	0.976
δ(WCO)	558 (551)	0.997	0.983
$W-C_{ax}$	465 (450)	0.991	0.965
$\nu(WC_{eq})$	452 (456)	1.002	1.010
$\delta(MCO_{ax})$	623 (612)	0.997	0.974
$\delta(MCO_{eq})$	527 (522)	0.998	0.988
ν_{as}(WC)	400 (413)	1.010	1.032
		$\prod$ EXC = 0.995	$\prod$ ZPE = 0.929

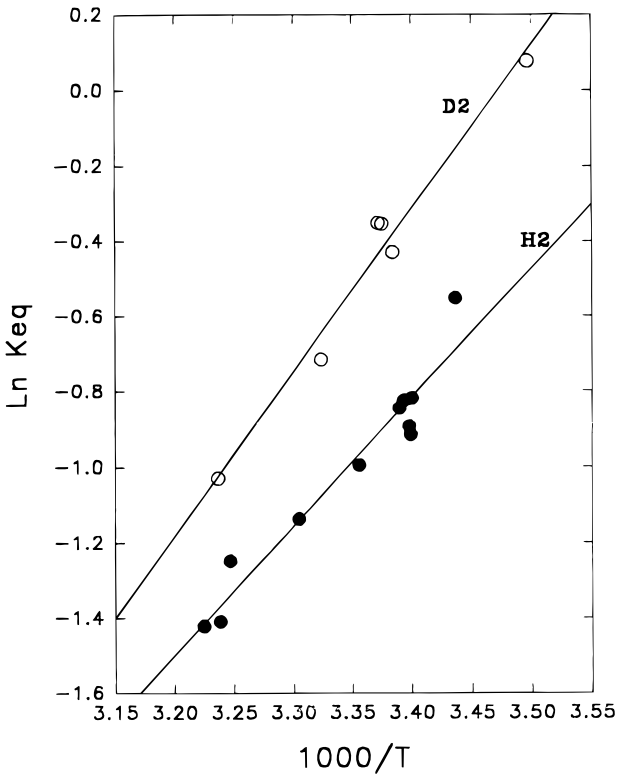

Figure 6. Plot of ln K_{eq} vs $1/T$ for the binding of H_2 and D_2 to Cr-$(CO)_3(PCy_3)_2$ in THF solution.

considerably lowered from that for unbound H_2 gas (4300 cm^{-1}). Table 7 lists all known vibrational data for H_2 complexes as well as H−H distances. The M−H_2 stretching and deformational modes have been less often reported, partly because of interference from coligands or in difficulty in assignment, especially if hydride ligands are also present. This was the case for Tp*RuH$(H_2)_2$ (Tp* = hydridotris(3,5-dimethylpyrazolyborate)), which showed four unassignable bands at 458−834 cm^{-1}.[4x] Recently near-IR laser Raman data were reported for [CpRu(dppm)(H_2)]BF_4[23] which included the lowest reported value for ν(HH), 2082 cm^{-1}, and also low-frequency RuH_2 vibrations and deformations (dppm = $Ph_2PCH_2PPh_2$). The reported assignments (as listed in Table 7) are questionable however, because the H−H bond is weak (d(HH) = 1.10 Å), which implies strong Ru−H bonds, yet the RuH_2 frequencies are among the lowest ever reported.

As expected there is generally a large dependence of the modes on both metal and ligand. However, vibrational analysis of a metal−η^2-H_2 system is complicated by the three-center, two-electron bonding. The bonding is essentially of the Dewar−Chatt−Duncanson type present in metal−olefin complexes, where there is a strong M→H_2 σ^* back-donation component, E_{BD}, to the bonding in addition to electron donation, E_D, to the empty metal d-orbital from the H_2 electron pair.

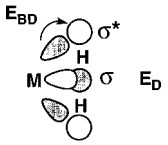

Theoretical calculations by Ziegler on **1** have shown that the E_{BD} component is energetically as strong as E_D, and up to twice as strong in other H_2 complexes with more phosphine donor ligands.[24] Back-bonding is much weaker in complexes with mostly π-acceptors, although the calculations[24a] show that E_{BD} in $Mo(CO)_5(H_2)$ still has about one-half the energy of E_D (ν-(CO) values also indicate H_2 is still a good π-acceptor here[4g]). One might anticipate a correlation of ν(HH) with the back-bonding ability (electron richness) of the metal center, as found for ν(NN) and ν(CO) in similar π-acceptor N_2 and CO ligands. The decrease in ν(HH) on going from $Mo(CO)_5(H_2)$ to Mo-$(CO)_3(PCy_3)_2(H_2)$ to $Mo(CO)(dppe)_2(H_2)$ at first glance does seem to reflect increased H−H bond weakening by the more electron-rich metal centers. However, ν(HH) decreases in the order Mo > Cr > W for $M(CO)_5(H_2)$, whereas Cr should be the worst back-bonder and give the highest ν(HH). The value of ν(HH) in $W(CO)_5(H_2)$ (2711 cm^{-1}) is far out of line with the much higher values in the Cr and Mo congeners (3030 and 3080 cm^{-1}) and also differs little (20 cm^{-1}) from that in vastly more electron rich $W(CO)_3(PCy_3)_2(H_2)$. The pentacarbonyl is unstable at room temperature and is presumed to have a shorter HH distance and a stronger H−H bond (although as discussed below such electrophilic metal centers may offset lower E_{BD} by higher E_D). In any event it is quite clear from the data in Table 7 that ν(HH) does not correlate well with H−H distance. Although the two complexes with the longest H−H separations (<1.1 Å) show the lowest ν(HH), these values are not that much lower than those for complexes considered to be "true" H_2 complexes with H−H distances less than 0.9 Å. This is mainly a result of the "give and take" bonding synergism here (E_D and E_{BD}), which represents concomitant formation of M−H bonds and cleavage of the H−H bond. Thus the HH stretch cannot be viewed as an isolated mode in H_2 complexes. The normal coordinate analysis of $W(CO)_3(PCy_3)_2(H_2)$ indeed treats the

(23) Chopra, M.; Wong, K. F.; Jia, G.; Yu, N.-T. *J. Mol. Struct.* **1996**, *379*, 93.

(24) (a) Li, J.; Ziegler, T. *Organometallics* **1996**, *15*, 11482. (b) Li, J.; Dickson, R. M.; Ziegler, T. *J. Am. Chem. Soc.* **1995**, *117*, 11482.

Table 7. IR Frequencies for ν(HH) and MH_2 Modes in Stable and Unstable Dihydrogen Complexes[a]

complex	ν(HH)	$\nu_{as}(MH_2)$	$\nu_s(MH_2)$	$\delta(MH_2)$	d(HH)[b]	ref
$CpV(CO)_3(H_2)$	2642					4s
$CpNb(CO)_3(H_2)$	2600					4s
$Cr(CO)_5(H_2)$	3030	1380	869, 878			4h,4y
$Cr(CO)_3(PCy_3)_2(H_2)$		1540	950	563[c]	0.85	4f
$Mo(CO)_5(H_2)$	3080					4h
$Mo(CO)_3(PCy_3)_2(H_2)$	~2950[d]	~1420[d]	885	471	0.87	3b
$Mo(CO)_3(PCy_2\text{-}i\text{-}Pr)_2(H_2)$			~870	~465		3b
$Mo(CO)(dppe)_2(H_2)$	2650		875		0.88	4j
$W(CO)_5(H_2)$	2711		919			4h
$W(CO)_4(C_2H_4)(H_2)$	2717					4t
$W(CO)_3(P\text{-}i\text{-}Pr_3)_2(H_2)$	2695	1567	953	465	0.89	3b
$W(CO)_3(PCy_3)_2(H_2)$	2690	1575	953	462	0.89	3b
$W(CO)_3(PCyp_3)_2(H_2)$		1565	938			4k
$W(CO)_3(PCy_2\text{-}i\text{-}Pr)_2(H_2)$		1570	937	456		3b
$MnCl(CO)_4(H_2)$		{1357, 1322}	764			4z
$MnBr(CO)_4(H_2)$		{1392, 1369}	789			4z
$Fe(CO)(NO)_2(H_2)$	2973	1374	~870			4l
$Co(CO)_2(NO)(H_2)$	{3100, 2976}[e]	1345	868			4l
$FeH_2(H_2)(PEtPh_2)_3$	2380		850	500, 405[f]	0.82[g]	4m
$RuH_2(H_2)(PMe_3)_3$	2360					4o
$[CpRu(dppm)(H_2)]^+$	2082	1358	679	486	1.10[h]	23
$Tp^*RuH(H_2)_2$	2361				0.90[i]	4x
$Tp^*RuH(H_2)(THT)$	2250				0.89[i]	4x
$[Os(NH_3)_5(H_2)]^{2+}$	2231				1.34[j]	4n
$Tp^*RhH_2(H_2)$	2238				0.94[k]	4p
$Pd(H_2)$			960			4r
$Ni(510)-(H_2)$[l]	3205	1185	670			4q

[a] Frequencies in cm^{-1}; complexes in italics are unstable at room temperature. Samples in mineral oil mulls for stable complexes and in liquid Xe or matrices for unstable species. Abbreviations: Cyp = cyclopentyl; Tp* = hydridotris(3,5-dimethylpyrazoylborate; dppm = $Ph_2PCH_2PPh_2$; THT = tetrahydrothiophene. [b] H−H distance in Å (solid state NMR distance from ref 4i except where noted). [c] Assignment unclear; could be $\delta(MH_2)_{out-of-plane}$. [d] Estimated from observed D_2 isotopomer bands. [e] Split possibly by Fermi resonance. [f] Assignment unclear (data from INS). [g] Neutron diffraction distance. Actual distance is undoubtedly longer when corrected for H_2 libration as in the case of the Mo−dppe complex (ref 4j). [h] For the Cp* analogue (ref 4u). [i] Calculated from T_1 data from solution NMR measurements. [j] For $[Os(ethylenediamine)_2(H_2)(acetate)]^+$ (ref 4v). [k] Calculated from inelastic neutron scattering data. [l] Data from EELS spectroscopy. H_2 believed to be bound in η^2 fashion on stepped edges of the Ni surface.

W−H_2 interaction as a triangulo system, i.e. where direct back-bonding electronic interactions exist between W and H atoms (below, left) rather than as the strictly 3-center bonding representation (below right).

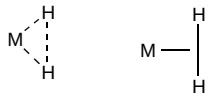

This is confirmed by the fact that the WH stretching force constant is as large as that for the HH stretch and that the HH, WH interaction is very large, indicating that stretching the HH bond leads to strengthening of WH, and vice versa. This extensive mixing along with the reduction of the ν(HH) force constant to one-fourth the value in free H_2 indicates that weakening of the H−H bond and formation of W−H bonds is already well along the reaction coordinate to oxidative addition in **1**. Furthermore, as the H−H bond becomes more activated (stretched) on a metal fragment, the observed ν(HH) mode will have increasing M−H character relative to H−H character. Upon H−H cleavage, this mode will then be assimilated into the M−H stretching mode, which generally occurs in the 1700−2300 cm^{-1} range. Thus the 2231-cm^{-1} frequency in Table 7 for the cationic Os complex with a very long H−H separation (<1.3 Å) probably should be thought more of as ν(OsH) than ν(HH). The frequency of this highly mixed mode could possibly go down then back up again on a given metal fragment as the H−H bond is activated and then broken by changing the ligand environment. This is overall an unprecedented situation in chemistry and vibrational spectroscopy. It would be most interesting to study the gradual activation of a series of M−η^2-HD complexes since ν(HD) and the two ν(M−HD) modes (the frequencies for all of which are intermediate in value to those for the H_2 and D_2 isotopomers) must eventually transform into two widely-separated M−H and M−D stretches. The question is how and at what point might this happen, given the continuum nature of the system.

Importantly, the force constant analysis appears to indicate that the H_2 ligand in **1** is further activated than may have been previously thought. It has always been a paradox that the H−H distances in **1** or any of the Group 6 complexes in Table 7 (0.85−0.89 Å, solid state NMR) are not as "stretched" as some of those found in later transition element complexes (1.0−1.5 Å),[4a−c] yet the H−H bond in **1** undergoes equilibrium cleavage in solution (eq 3). Thus the H−H distance may not always reflect the degree of "readiness to break", i.e. a very late transition state may exist. At the other end of the spectrum, for $W(CO)_5(H_2)$ and other highly electrophilic complexes, the T-shaped entity pictured above with one internal coordinate, the H−H stretch, may be a more appropriate model for vibrational analysis, as mentioned in a footnote in Poliakoff's paper.[4h] However, it is difficult to draw the line on which analysis should be applied because some degree of back-bonding and incipient M−H bond formation will always be present. Furthermore, the T-shaped bonding that represents the purely three-center interaction (E_D) in σ complexes can be reasonably strong by itself in the absence of much back-bonding. The Lewis-base type interaction of H_2 with a highly electrophilic metal center (Lewis acid) has a much stronger E_D than with a more electron-rich metal center, and this can completely offset the lower E_{BD}. For example, the cationic H_2 complex $[Mn(CO)(dppe)_2(H_2)]^+$ has remarkably similar properties, e.g. H−H distance and J_{HD}, to its isoelectronic neutral analogue, $Mo(CO)(dppe)_2(H_2)$.[4w] In the case of electrophilic cationic complexes,

the H−H bond can be considerably weakened (although cannot be broken) by the E_D bonding component alone without much back-bonding from the metal.

The lack of reliable correlation of vibrational versus other properties brought about by the bonding complexities extends to the M−H_2 modes. These also show metal/ligand dependence, though to a lesser degree than ν(HH) (Table 7). $\nu_s(MH_2)$ is ~70 cm^{-1} lower in $Mo(CO)_3(PCy_3)_2(H_2)$ than in the W congener (**1**), which combined with the higher ν(HH) for the Mo species suggests weaker coordination of H_2 to Mo than W. This correlates well with the known thermal stabilities. The $\nu_s(MH_2)$ and $\nu_{as}(MH_2)$ values for the *unstable* W, Fe, Co carbonyl and Pd(H_2) species are also lower than those for stable **1**. However, one would have anticipated $\nu_s(MH_2)$ to be appreciably higher for **1** than for its Cr analogue because of the higher M−H_2 binding energy measured for **1** and the far greater stability of **1** to H_2 dissociation in solution.[4f] The frequencies were nearly identical, however, and a minor ligand change from PCy_3 to tricyclopentylphosphine affected $\nu_s(MH_2)$ more than changing the metal. Also $\nu_s(MH_2)$ values are nearly identical for $Mo(CO)_3(PCy_3)_2(H_2)$ and $Mo(CO)(dppe)_2(H_2)$ though ν(HH) is 300 cm^{-1} lower for the latter. As is the case for ν(HH), the metal−hydrogen stretching frequencies represent an inseparable combination of MH *and* HH interactions.

Experimentally Determined Equilibrium Isotope Effects (EIE's). Measurements of the EIE values for the Cr and W complexes (made after the calculations had been performed) agree within experimental error with the calculated value of 0.78 for eq 6. It should be noted that the measured equilibrium constants are K_p values expressed in terms of the pressure of $H_2(D_2)$ above the solution. Care was taken to make sure that the solvent was saturated with H_2 or D_2. What limited data are available indicate that D_2 is about 3% more soluble than H_2 in water and common organic solvents.[25] Accurate values for the solubility of D_2 in THF were not found, so the activity of the gas is used in all equilibrium expressions.

$$Cr(CO)_3(PCy_3)_2(D_2) + H_2 \overset{K_{H/D}}{\rightleftharpoons} Cr(CO)_3(PCy_3)_2(H_2) + D_2 \quad (16)$$

Division of eq 13 by eq 14 gives eq 16, the EIE for the binding of H_2 vs D_2 to $Cr(CO)_3(P(Cy)_3)_2$ in solution. The experimental EIE was determined from the equilibrium data for the binding of H_2 and D_2 to the chromium complex $Cr(CO)_3(PCy_3)_2$ (eqs 13 and 14). The inverse EIE ($K_{H/D} = 0.65 \pm 0.15$ at 22 °C for eq 16) arises from an unfavorable enthalpy term, $\Delta\Delta H = 1.8 \pm 1.0$ kcal mol^{-1}, overcoming a favorable entropy term, $\Delta\Delta S = 5.3 \pm 4.0$ cal mol^{-1} deg^{-1}.[26] The standard entropy of D_2 gas (34.6 cal mol^{-1} deg^{-1})[27] is 3.4 cal mol^{-1} deg^{-1} more positive than that of H_2 gas (31.2 cal mol^{-1} deg^{-1}); the more negative entropy of binding of D_2 gas is due to the greater loss of rotational and translational entropy for the heavier D_2.

In light of the fact that the free D−D bond is 1.8 kcal mol^{-1} *stronger* than the H−H bond, a naive view would be to expect H_2 to bind preferentially. Thus if the W(D_2) and W(H_2) bonds were of equal strength, eq 6 would be predicted to be exothermic by −1.8 kcal mol^{-1} based on the fact that the D−D bond is that much stronger. The more negative enthalpy of binding D_2 more than overcomes the unfavorable entropic barrier and is responsible for the preferred binding of D_2 (and the inverse EIE in eq 16). The fact that, for the chromium complex at least, the analogue of reaction 6 is actually endothermic by this amount implies that zero-point (and excited state) vibrational energies for the dihydrogen species determine the EIE.

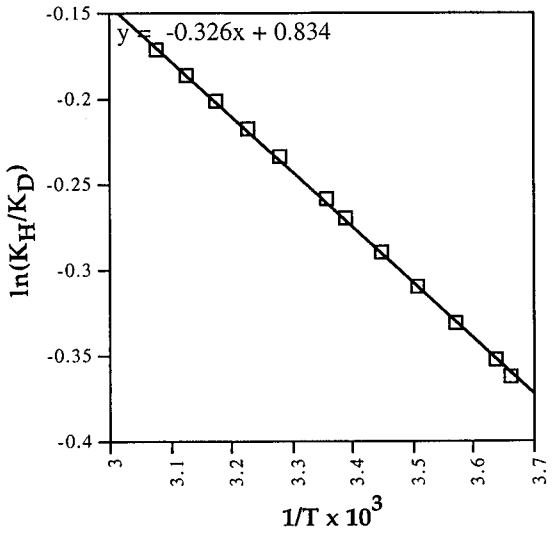

Figure 7. Plot of $\ln(K_H/K_D)$ vs $1/T$ for the EIE calculated from vibrational data.

Enthalpic Origin of the Deuterium EIE for Binding of Dihydrogen to a Molecular Hydrogen Complex. Relative enthalpic and entropic contributions to the calculated equilibrium in eq 6 were obtained from a plot of calculated $\ln(K_H/K_D)$ values vs $1/T$, Figure 7. We obtained ΔH and ΔS for the equilibrium in eq 6 from the slope and intercept of this line. These results gave a small positive ΔH of 0.64 kcal mol^{-1} and a ΔS term of 1.7 cal mol^{-1} deg^{-1} for eq 6. These calculated thermodynamic parameters for the tungsten system may be judiciously compared to the corresponding measured parameters for the Cr analog: $\Delta\Delta H = 1.8$ kcal mol^{-1}; $\Delta\Delta S = 5.3$ cal mol^{-1} deg^{-1}. The calculated tungsten values differ slightly in magnitude from those measured for the Cr case; however, in both cases, an unfavorable enthalpy term overcomes a favorable entropy term. *Thus D_2 binds better for enthalpic reasons, even though the complexation of D_2 is disfavored entropically.*

The equilibrium isotope effect for both dissociative and nondissociative addition of H_2 to metal complexes in solution has been studied by several groups,[2] and the results of a few recent studies are summarized in Table 8. For more meaningful comparison, we have used the authors' Arrhenius parameters to calculate EIE's at the common temperature of 300 K.

All of the entries in Table 8 show inverse EIE's for the binding of H_2 vs D_2, and their corresponding measured Arrhenius parameters reveal that in each case D_2 binding is enthalpically favored over H_2 binding, while D_2 binding is disfavored entropically. It should be pointed out that two entries in Table 8 contain contributions from α and β secondary deuterium effects. The first entry, Bergman's heterobimetallic Ta−Ir complex, contains bridging $CH_2(CD_2)$ ligands which contribute a β-secondary effect to the observed EIE. Caulton's Ir(III) complex, entry 3, is the measured EIE for the binding of H_2 vs D_2 to the corresponding hydride and deuteride complexes. Thus the measured EIE contains an α secondary effect. Goldman and Krogh-Jespersen have estimated the magnitudes of such α and β secondary effects for the addition of H_2/D_2 to MX and $M(CX_3)$ (X = H, D) model complexes. These studies give normalized α and β secondary effects of 0.88 and 0.84 (at 300 K). Correcting Bergman's and Caulton's EIE would decrease the apparent EIE's (make them slightly less inverse)

(25) Cook, M. W.; Hanson, D. N.; Alder, B. J. *J. Chem. Phys.* **1957**, *26*, 748.

(26) The $\Delta\Delta H$ for eq 16 is ΔH(eq 13) − ΔH(eq 14) = −6.8 −(−8.6) kcal mol^{-1}. The $\Delta\Delta S$ for eq 16 is ΔS(eq 13) − ΔS(eq 14) = −24.7 − (−30.0) cal mol^{-1} deg^{-1}.

(27) *Handbook of Chemistry and Physics*, 62nd ed.; Weast., R. C., Ed.; CRC Press: Boca Raton, FL, 1981−82; Table F-203.

Table 8. Comparison of Thermodynamic Parameters for the Binding of H_2 and D_2 to Various Metal Complexes

K_{eq}	ΔH (kcal/mol)	ΔS (cal/(mol deg))	EIE	ref
$[Cp_2Ta(\mu\text{-}CH_2)_2Ir(CO)_2(H)_2]/\{[H_2][Cp_2Ta(\mu\text{-}CH_2)_2Ir(CO)_2]\}$	−12.0 (0.2)	−23.7 (0.6)	0.56[a]	2a
$[Cp_2Ta(\mu\text{-}CD_2)_2Ir(CO)_2(D)_2]/\{[D_2]\ [Cp_2Ta(\mu\text{-}CD_2)_2Ir(CO)_2]\}$	−13.0 (0.4)	−25.9 (1.2)		
$[W(H)_2L_4I_2]/\{[H_2]\ [WL_4I_2]\}$	−19.7 (0.6)	−45 (2)	0.85[a]	
$[W(D)_2L_4I_2]/\{[D_2]\ [WL_4I_2]\}$	−21.6 (0.7)	−51 (3)		
$[Ir(H)_2Cl(L)_2(H_2)]/\{[H_2]\ [Ir(H)_2Cl(L)_2]\}$	−6.8 (0.2)	−19.2 (0.7)	0.47[a]	2e
$[Ir(D)_2Cl(L)_2(D_2)]/\{[D_2][Ir(D)_2Cl(L)_2]\}$	−7.7 (0.5)	−20.7 (1.8)		
$[Cr(H_2)L_2(CO)_3]/\{[H_2]\ [CrL_2(CO)_3]\}$	−6.8 (0.5)	−25 (2)	0.70[a]	this work
$[Cr(D_2)L_2(CO)_3]/\{[D_2]\ [CrL_2(CO)_3]\}$	−8.6 (0.5)	−30 (2)		

[a] EIE calculated from Arrhenius parameters at 300 K.

and bring them closer to the measured and calculated values for our Cr/W dihydrogen case.

Goldman and Krogh-Jespersen clarified the vibrational origin of "inverse" EIE's for both solution dihydride cases cited in Table 8. As part of a more general examination of primary and secondary isotope effects for dihydrogen and alkane addition to metal complexes,[2c] they measured and calculated the EIE for the addition of H_2 and D_2 to a Vaska's type complex, *trans*-$Ir(CO)L_2Cl$ (eq 17 and 18). Dividing eq 17 by eq 18 gives eq 19, an expression for the EIE.

$$(L)_2Ir(CO)Cl + H_2 \overset{K_H}{\rightleftharpoons} (L)_2Ir(H)_2(CO)Cl \qquad (17)$$

$$(L)_2Ir(CO)Cl + D_2 \overset{K_D}{\rightleftharpoons} (L)_2Ir(D)_2(CO)Cl \qquad (18)$$

$$H_2 + \underset{\textbf{3-}d_2}{(L)_2Ir(D)_2(CO)Cl} \overset{K_H/K_D}{\rightleftharpoons} D_2 + \underset{\textbf{3}}{(L)_2Ir(H)_2(CO)Cl} \qquad (19)$$

The measured EIE[2c] for eq 19 ($L = PPh_3$) was inverse: $K_H/K_D = 0.55(6)$ at ambient temperature; a similar EIE was calculated from computed vibrational frequencies ($L = PH_3$, $K_H/K_D = 0.46$ at 300 K). Thus both theory and experiment concur that D_2 binds better than H_2 to Vaska's complex. The calculated values, $\Delta\Delta H° = 1.14$ kcal mol^{-1} and $\Delta\Delta S^o = 2.28$ cal mol^{-1} deg^{-1}, for eq 23 are in good agreement with those measured experimentally by Werneke and Vaska:[28] $\Delta\Delta H° = 0.8$ kcal mol^{-1} and $\Delta\Delta S^o = 2.0$ eu (no errors given).

When H_2 (or D_2) forms a dihydride complex, the combined inverse ZPE and EXC contributions from new isotope sensitive vibrational modes overcome the normal ZPE contribution from the HH (DD) stretch *and* rotational effects which oppose the observed inverse EIE.[2c] This conclusion provided the first theoretical explanation of Bergman's[2a] and Parkin's[2b] observed inverse effects, and is *the* important precedent for our analysis of the EIE for the binding of H_2/D_2 in a molecular hydrogen complex. More recently, the importance of new isotope-sensitive vibrational modes in the complexation of alkenes[29] and alkanes[30] to transition-metal complexes has been reported and discussed.

In Table 9 we have compared our calculated enthalpy and entropy terms from the EIE temperature dependence for the formation of a dihydrogen complex to those calculated by Krogh-Jespersen and Goldman[2c] for the formation of a dihydride

Table 9. Comparison of Calculated Thermodynamic Parameters for Deuterium EIE's

K_H/K_D	MMI	EXC	ZPE	EIE	$\Delta\Delta H°$ (kcal mol^{-1})	$\Delta\Delta S°$ (cal deg^{-1} mol^{-1})
$\{[D_2]\ [\textbf{3}]\}/\{[H_2][\textbf{3-}d_2]\}$	5.66[a]	0.84[a]	0.10[a]	0.46[a]	1.15	2.28
$\{[D_2]\ [\textbf{1}]\}/\{[H_2][\textbf{1-}d_2]\}$	5.77[b]	0.67[b]	0.20[b]	0.78[b]	0.64	1.7

[a] Data from ref 2c; EIE data calculated at 300 K. [b] This work; EIE data calculated at 300 K.

(the EIE's were calculated over the same temperature range: 280 to 320 K).

Finally, we note that the calculated and measured EIE for binding of H_2 vs D_2 to the tungsten dihydrogen complex **1** is a factor of 1.7 less "inverse" than the corresponding EIE calculated and measured by Krogh-Jespersen and Goldman for the binding of H_2/D_2 to Vaska's complex—this difference has important implications for the predicted and measured EIE for tautomerization equilibria like those in eqs 3 and 20.

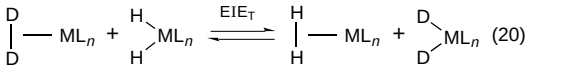

If we assume that the EIE for eq 6 is typical for the nonclassical $M(H_2)$ case and that the EIE of eq 19 is typical for a classical $M(H)_2$ case, we may estimate the EIE for the tautomerization in eq 20: $EIE_T = EIE(eq\ 6)/EIE(eq\ 19)$. Using the calculated EIE's for eq 6 (0.78) and that for eq 19 (0.45), we predict that the EIE in eq 20 is "normal"—i.e., that deuterium favors the classical site *at 300 K*.

Because the MMI factors are (and should be) similar for eqs 6 and 19 (ΔS for eq 20 is negligible), the predicted preference for deuterium in the classical tautomer may be traced to the more "inverse" ZPE factor for eq 19 (0.10) versus the corresponding ZPE factor for eq 6 (0.20, see Table 9). Because ΔZPE changes for the dihydride and molecular hydrogen cases are both referenced to free $H_2(D_2)$, we conclude that *changes* in MH_2 force constants between tautomers (not the conversion of molecular translations and rotations into vibrations) lead to the predicted preference of deuterium in the dihydride tautomer. This reasoning is also consistent with an increase in the corresponding force constants for low-frequency modes when the "loose" $M(H_2)$ fully adds (despite the weakening of the bound HH(DD) force constant). Indeed the predicted preference of deuterium in the dihydride tautomer merely parallels (but for different reasons) the preference of deuterium in a complex versus as a free, unbound molecule.

Because we do not have vibrational frequencies for the "classical" dihydride tautomer of **1** and **1**-d_2, we cannot test our predicted EIE for the $W(CO)_3L_2(H)_2/W(CO)_3L_2(H_2)$ tautomeric equilibrium in eq 20. The predicted "normal" EIE for eq 20 is supported by the corresponding "normal" KIE for conversion of classical to nonclassical tautomers measured

(28) Werneke, M. F. Ph.D. Thesis, Clarkson College of Technology, 1971. Results quoted from ref 2c.

(29) Bender, B. R. *J. Am. Chem. Soc.* **1995**, *117*, 11239.

(30) (a) Bengali, A. A.; Arndtsen, B. A.; Burger, P. M.; Schultz, R. H.; Weiller, Kyle, K. R.; Moore, C. B.; Bergman, R. G. *Pure Appl. Chem.* **1995**, *67*, 281. (b) Schultz, R. H.; Bengali, A. A.; Tauber, M. J.; Weiller, B. H.; Wasserman, E. P.; Kyle, K. R.; Moore, C. B.; Bergman, R. G. *J. Am. Chem. Soc.* **1994**, *116*, 7369. (c) Bengali, A. A.; Schultz, R. H.; Moore, C. B.; Tauber, M. J.; Weiller, B. H.; Wasserman, E. P.; Kyle, K. R.; Bergman, R. G. *J. Am. Chem. Soc.* **1994**, *116*, 9585.

earlier by some of us.[31] EIE's for equilibria like that of eq 20 have been reported, but the conclusions diverge: Luo and Crabtree reported[32] that deuterium favors the nonclassical site in $[ReH_2(H_2)(CO)L_3]^+$; Poliakoff and co-workers also found[33] that deuterium favors the nonclassical site in $CpNb(CO)_3(H_2)$ versus $CpNb(CO)_3H_2$. On the other hand, Heinekey and Oldham found[34] that deuterium favors the classical site in $[Cp^*IrL(H)(H_2)]^+$ and Henderson and Oglieve reported[35] that deuterium favors the classical tautomer in the complex $[Cp_2WH_2]^+$. In light of the fact that these studies ranged over very different temperatures, we think it unwise to state a general rule concerning whether deuterium favors a classical versus a nonclassical site.

Conclusions

A normal coordinate analysis has been performed on $W(CO)_3(PCy_3)_2(H_2)$ (**1**) and its isotopomers with HD (**1**-d_1) and D_2 (**1**-d_2). The major revelation was the high extent of mixing between the HH stretch and the WH_2 modes, where in fact the WH stretching force constant is as large as that for the HH stretch. The frequency of the HH stretch in H_2 complexes would thus not be expected to be a reliable predictor of HH bond length, bond strength, or any related parameter. The force constant for the HH stretch, 1.3 mdyn/Å, is less than one-fourth the value in free H_2. This indicates that weakening of the H−H bond and formation of W−H bonds are quite far along the reaction coordinate to oxidative addition even in "true" H_2 complexes that possess the shortest measured H−H distances (0.85−0.89 Å, solid state NMR). The two-dimensional nature of the reaction coordinate which involves coupling of H−H and M−H modes is an intriguing problem for future study.

Using the vibrational modes established for **1** and **1**-d_2, we have calculated the deuterium equilibrium isotope effect for the binding of H_2 and D_2 to **1** and **1**-d_2. The calculated EIE is inverse (D_2 is bound better than H_2), and a detailed consideration of component factors shows that zero-point energy contributions from five new vibrational modes and Boltzmann excitation contributions[36] from new low-frequency modes oppose and overcome a large mass and moment (MMI) factor and a large zero-point energy (ZPE) factor change for the HH stretch, much like the case for the addition of H_2 to metal complexes to form dihydrides. We also have calculated the enthalpy and entropy parameters associated with the temperature dependence of the EIE.

We have experimentally confirmed the calculated "inverse" equilibrium isotope effect for the binding of H_2 and D_2 to $W(CO)_3(PCy_3)_2$ and $Cr(CO)_3(PCy_3)_2$ in solution. The preferred binding of D_2 versus H_2 is enthalpic in nature in accord with our analysis of the same EIE from measured vibrational frequencies of **1** and **1**-d_2. Conceptually it should thus be possible to separate hydrogen isotopes, including tritium, at *room temperature* on metal complexes that reversibly bind H_2 *molecularly* (hydrides will give exchange), using for example cationic complexes supported on alumina. The separation factors calculated for H_2/D_2 and eight other[37] mixed H−D−T isotopomeric combinations on $W(CO)_3(PCy_3)_2$ at 25 °C are generally better than those at the cryogenic temperatures (ca. −150 °C) currently used for such separations on alumina-type supports.

Acknowledgment. We dedicate this work to Jacob Bigeleisen and to the memory of Maria Goeppert-Mayer on the 50th anniversary of the publication of their general treatment of equilibrium isotope effects (ref 6). The authors thank Jacob Bigeleisen and Alan Goldman for helpful discussions. B.R.B. thanks Rick Finke for indirect financial support of this research. G.J.K. acknowledges funding support by the Department of Energy, Office of Basic Energy Sciences, Division of Chemical Sciences. This work has also benefitted from the use of facilities at the Manuel Lujan Jr. Neutron Scattering Center, a National User Facility funded as such by the Department of Energy, Office of Basic Energy Sciences.

JA971009C

(31) Zhang, K.; Gonzalez, A. A.; Hoff, C. D. *J. Am. Chem. Soc*. **1989**, *111*, 3628.

(32) Luo, X.-L.; Crabtree, R. H. *J. Am. Chem. Soc*. **1990**, *112*, 6912.

(33) Haward, M. T.; George, M. W.; Hamley, P.; Poliakoff, M. *J. Chem. Soc., Chem. Commun*. **1991**, 1101.

(34) Heinekey, D. M.; Oldham, W. J., Jr. *J. Am. Chem. Soc*. **1994**, *116*, 3137.

(35) Henderson, R. A.; Oglieve, K. E. *J. Chem. Soc., Dalton Trans* **1993**, 3431.

(36) Another point evident from our comparison is that the EXC term for the molecular hydrogen case is less than that for the dihydride case (0.68 vs 0.84). The greater deviation from unity for the molecular hydrogen case arises from the presence of more low-frequency isotope sensitive modes (hence more excited states) in the molecular hydrogen case than in the dihydride case. Bergman has called attention to the presence of such low-frequency modes in alkane σ-complexes and their contributions to observed "inverse" EIE's for alkane complex equilibria at low temperatures (see ref 30c).

(37) King, W. A.; Kubas, G. J. Unpublished results.